Available online at www.sciencedirect.com
SCIENCE DIRECT
Tetrahedron
Tetrahedron 61 (2005) 5089–5100

Molecular recognition of biotin, barbital and tolbutamide with new synthetic receptors

Rosa M. Claramunt,[a,*] Fernando Herranz,[a] M. Dolores Santa María,[a] Elena Pinilla,[b] M. Rosario Torres[b] and José Elguero[c]

[a]*Departamento de Química Orgánica y Bio-Orgánica, UNED, Facultad de Ciencias, Senda del Rey 9, E-28040 Madrid, Spain*
[b]*Laboratorio de Difracción de Rayos X, Departamento de Química Inorgánica, Facultad de Ciencias Químicas, Universidad Complutense, E-28040 Madrid, Spain*
[c]*Instituto de Química Médica, Centro de Química Orgánica 'Manuel Lora-Tamayo', C.S.I.C., Juan de la Cierva 3, E-28006 Madrid, Spain*

Received 14 January 2005; revised 4 March 2005; accepted 7 March 2005

Available online 19 April 2005

Dedicated to our friend Dr. Carmela Ochoa de Ocáriz on her 65th anniversary

Abstract—We have measured, by means of NMR titrations, the binding constants for the complexes between hosts *N*,*N*′-bis(6-methylpyridin-2-yl)-1,3-benzenedicarboxamide (**7**) and 4-chloro-*N*,*N*′-bis(6-methylpyridin-2-yl)-2,6-pyridinedicarboxamide (**8**, hydrated) with biotin methyl ester (**1**), *N*,*N*′-dimethylurea (**2**), 2-imidazolidone (**3**), *N*,*N*′-trimethylenurea (**4**), barbital (**5**) and tolbutamide (**6**) as guests. Molecular Mechanics calculations (Monte Carlo Conformational Search, AMBER and OPLS force fields, MacroModel v.8.1) on the complexes formed between the foregoing guests and hosts **7** and **8**, comparatively with 4-oxo-*N*,*N*′-bis(6-methylpyridin-2-yl)-1,4-dihydro-2,6-pyridinedicarboxamide (**9a**) have been carried out in order to determine the correlation between experimental and theoretical results and to understand the behaviour of the designed new hosts. Finally we have performed single point DFT [B3LYP/6-31G(d,p)] calculations on the optimised Molecular Mechanics geometries for the complexes between hosts **7**–**9** and water.

1. Introduction

In a preceding paper we have started the systematic study of host–guest complexes using guests of biological interest, with the final purpose to mimic the function of natural receptors by means of an iterative optimisation approach.[1] In that work we used two known hosts, those of Thummel[2] and Goswami[3] (Scheme 1) and five urea derivatives (the first five ones of the present work, biotin methyl ester (**1**), *N*,*N*′-dimethylurea (**2**), 2-imidazolidone (**3**), *N*,*N*′-trimethylenurea (**4**) and barbital (**5**) (Scheme 2).

Now we present our results on the interaction of two new hosts, *N*,*N*′-bis(6-methylpyridin-2-yl)-1,3-benzenedicarboxamide (**7**) and 4-chloro-*N*,*N*′-bis(6-methylpyridin-2-yl)-2,6-pyridinedicarboxamide (**8**), with six guests **1**–**6** (Scheme 2) adding to the previous list,[1] a sulfonyl urea, the anti-diabetic oral hypoglycaemic agent tolbutamide (**6**).[4] Even if our attempts to prepare host 4-oxo-*N*,*N*′-bis-

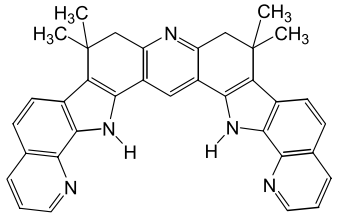

Thummel's host

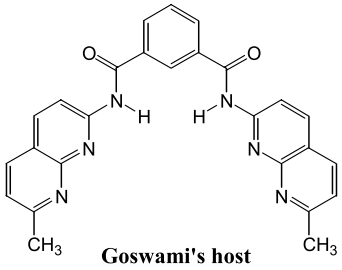

Goswami's host

Scheme 1. Thummel's and Goswami's hosts.

Keywords: Molecular recognition; Binding constants; Molecular modelling; NMR titrations.
* Corresponding author. Tel.: +34 91 3987322; fax: +34 91 3986697; e-mail: rclaramunt@ccia.uned.es

0040–4020/$ - see front matter © 2005 Elsevier Ltd. All rights reserved.
doi:10.1016/j.tet.2005.03.025

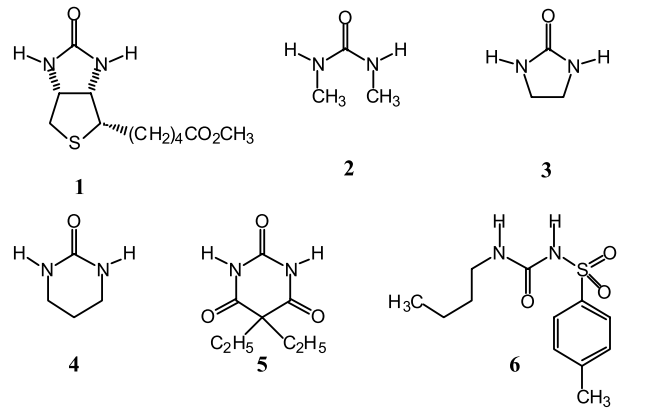

Scheme 2. The six guests (*N*,*N*′-dimethylurea is represented in the *E*,*E* conformation).

(6-methylpyridin-2-yl)-1,4-dihydro-2,6-pyridinedicarboxamide (**9a**) have been unsuccessful, we have studied its properties theoretically in comparison with hosts **7** and **8**.

^{1}H NMR titrations have been performed to measure and analyse the binding constants (K_b) of all guests with host **7** by a direct method,[1] using the Chemical Induced Shifts (CIS) on the 2-CH benzenic proton and the NHs of the 1,3-dicarboxamide groups. The same method was employed for complexes **8**:water and **8**:**1**, where the CIS on the NHs of the 2,6-pyridinedicarboxamides were quantified. The competitive method was needed to determine K_b in complexes of **8** and the remaining guests **2**–**6** measuring the NH-CIS of the urea moieties and the H_2O-CIS.[5]

All complexes have been modelled at different theoretical levels using the Monte Carlo conformational search with both AMBER and OPLS Force Fields (MacroModel v.8.1). We have carried out single point calculations at B3LYP/ 6-31G(d,p) level on the optimised Molecular Mechanics geometries (AMBER Force Field) for the complexes between hosts **7**, **8** and the two tautomers **9a** and **9b** with water (Scheme 3). The pyridone/hydroxypyridine tautomerism in **9** has also been approached with two models **10a** and **10b** at the B3LYP/ 6-31G(d,p) level but with complete optimisation of the geometry.

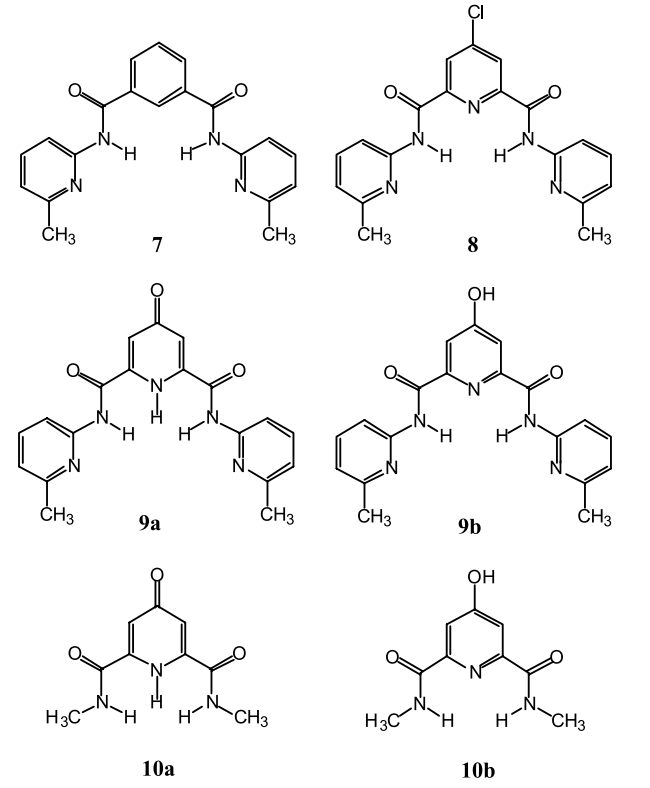

Scheme 3. Hosts **7**, **8** and **9** and model compound **10**.

2. Results and discussion

2.1. Chemistry

N,*N*′-Bis(6-methylpyridin-2-yl)-1,3-benzenedicarboxamide (**7**) was prepared according to Scheme 4 by condensation reaction of isophthaloyl chloride (**11**) with 2-amino-6-methylpyridine (**12**).[3]

The various attempts to obtain host **9** resulted in the synthesis of **8** (Scheme 5). 4-Oxo-1,4-dihydro-2,6-pyridinedicarboxylic acid or chelidamic acid (**13**) was treated with thionyl chloride to yield only 4-chloro-2,6-pyridinedicarbonyl dichloride (**15**),[6] being unable to reproduce the literature results where a mixture of **14** with **15** was formed and used without isolation to obtain several dicarboxamides.[7]

We also prepared the diethyl ester **16** from chelidamic acid **13** and ethyl orthoformate in acetic acid which would be further reacted with **12**, but the condensation between the ester and the amine did not occur. Other assays were the reaction of chelidamic acid **13** with 2-amino-6-methylpyridine (**12**) in the presence of several dehydrating agents (EDC/DMAP, DCC/DMAP) in different conditions but no signals attributable to **9** were apparent in the ^{1}H NMR spectra.

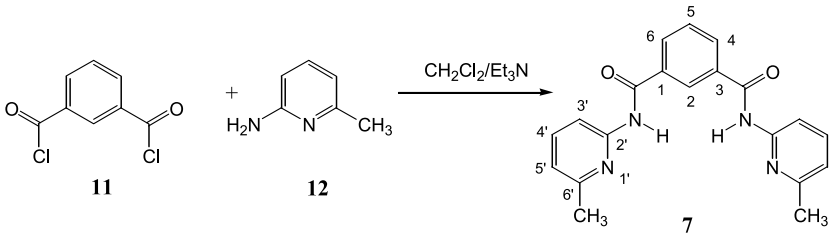

Scheme 4. Synthesis of host **7** from isophthaloyl chloride (**11**) and 2-amino-6-methylpyridine (**12**).

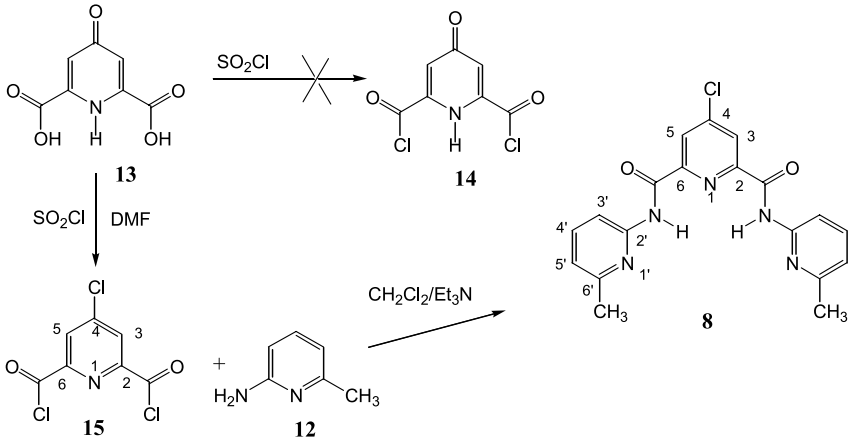

Scheme 5. Synthesis of host **8** from chelidamic acid (**13**) and 2-amino-6-methylpyridine (**12**).

Table 1. Experimental binding constants (M^{-1}) for complexes of host **7**

Guest	K_b (20–80%) 2-CH CIS	K_b (20–80%) NH CIS	Average K_b	ΔG (kJ mol^{-1})
1	950±86	1000±62	975	−17.2
2	≤10 [a]	≤10[a]	≤10	−4.0[b]
3	1400±85	1500±90	1450	−18.1
4	2250±353	2350±412	2300	−19.3
5	2442±384	2308±294	2375	−19.4
6	[c]	600±125	600	−15.9

[a] No CIS were observed.
[b] Calculated from $K_b=5$.
[c] No CIS was observed on the 2-CH proton.

Table 2. Experimental binding constants (M^{-1}) for complexes of host **8**

Guest	K_b (20–80%)	Round K_b	ΔG (kJ mol^{-1})
Water	93±10[a]	95	−11.4
1	3600±640[b]	3600	−20.4
2[c,d]	≤10	≤10	−4.0[c]
3	141±25[d]	140	−12.3
4	100±18[d]	100	−11.5
5	274±74[d]	275	−14.0
6	735±207[d]	735	−16.5

[a] Direct titration measuring the NH-CIS of the host **8**.
[b] Direct titration measuring the NH-CIS of the host **8**, the biotin NH chemical shifts do not change on complexation.
[c] Calculated from $K_b=5$. No CIS was observed.
[d] Competitive titration measuring the NH-CIS of the urea derivative and H_2O protons.

Table 3. Interaction energy values ($-E_{min}$ in kJ mol^{-1}) obtained with AMBER

Guest	**7**	**8**	**8**[a]	**9a**
1	60.7	69.3	71.6	58.6
(*E*,*E*)-**2**	29.0	31.5	23.0	43.0
(*Z*,*E*)-**2**	47.8	51.3	44.4	37.2
(*Z*,*Z*)-**2**	47.8	48.9	44.2	39.0
3	51.7	49.2	38.5	43.1
4	53.0	51.3	41.1	44.6
5	65.0	75.4	62.8	68.3
6	63.4[b]	107.8	84.2	72.6

[a] With the GB/SA model for water.
[b] This value has been calculated taking into account the real interactions in the **7/6** complex where only the SO_2–NH intervenes, on the basis of NOESY experiments. There is a minimum energy value for a theoretical complex that considers both urea NHs with a $-E_{min}$ in kJ mol^{-1} of 73.4.

2.2. Binding constants

The experimental binding constants (M^{-1}) measured in $CDCl_3$ at 300 K for complexes of the six guests **1–6** with host **7** are gathered in Table 1, and in Table 2 that with host **8** plus the measured binding constant **8**:water. The interaction energies of the process ($-E_{min}$ in kJ mol^{-1}) evaluated by Molecular Mechanics calculations for hosts **7**, **8** and **9a** with AMBER force field are shown in Table 3 and with OPLS force field in Table 4. As usual with this kind of studies, entropy changes have been assumed to be the same or rather close for all series.[1]

Special mention deserves the case of *N*,*N*′-dimethylurea **2**. For both hosts **7** and **8** we have failed to measure CIS with this guest. To determine values of K_b lower than 10 M^{-1} it would be necessary to use very concentrated solutions, 0.2 M or larger, thus preventing to attain the 20–80% saturation range in the titration procedure. Therefore, we

Table 4. Interaction energy values ($-E_{min}$ in kJ mol^{-1}) obtained with OPLS

Guest	**7**	**8**	**9a**
1	92.4	98.3	84.4
(*E*,*E*)-**2**	56.0	58.0	43.1
(*Z*,*E*)-**2**	70.4	68.0	59.4
(*Z*,*Z*)-**2**	57.5	56.3	42.6
3	80.3	77.0	53.2
4	81.7	81.0	55.6
5	92.5	101.5	73.2
6[a]	—	—	—

[a] Lack of parameters in OPLS force field for this compound.

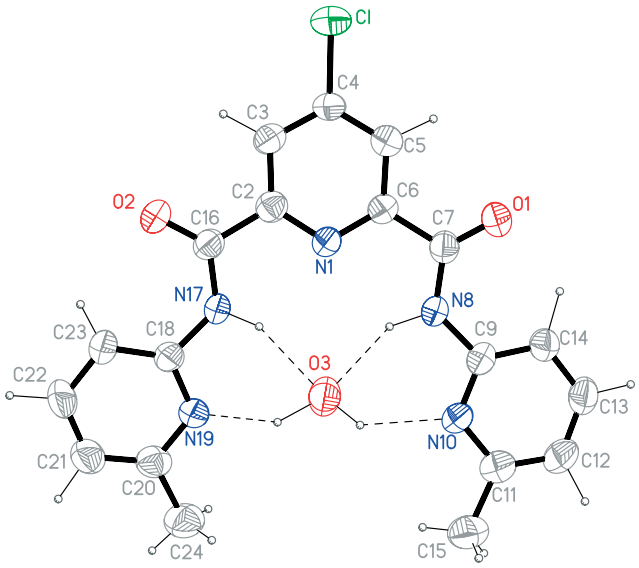

Figure 1. The X-ray structure of host **8** including a water molecule as a guest.

have indicated in Tables 1 and 2 a value of ≤ 10. We do not know the actual value (that can be different for **7** and **8**) of K_b, somewhere between near 0 and 10, so we have decided to adopt $K_b=5$ in both cases as a working hypothesis. Using other values such as $K_b=1$ or $K_b=0.1$, the conclusions do not change very much only the correlations slightly worsened.

We have represented in Fig. 1 the X-ray structure of **8**:H_2O. The crystal consists of molecules bonded through hydrogen bonds to water molecules. The **8**:H_2O entity is almost coplanar, the maximum dihedral angle between the pyridine rings on the 2,6-dicarboxamide nitrogens is 12.1 (1)°, and the oxygen atom O3 is located 0.543(3) Å out the least square plane formed by N10–N8–N17–N19 atoms. In addition, these entities (**8**:H_2O) are bonded with the centrosymmetric ones through C3–H3···O2 ($-x+1$, $-y+2$,$-z+2$) forming dimers, which are arranged in chains via C21–H21···O1 ($x-1$,$y-1$,z). These hydrogen bonds give rise to a ribbon of 19.22 Å width as depicted in Fig. 2.

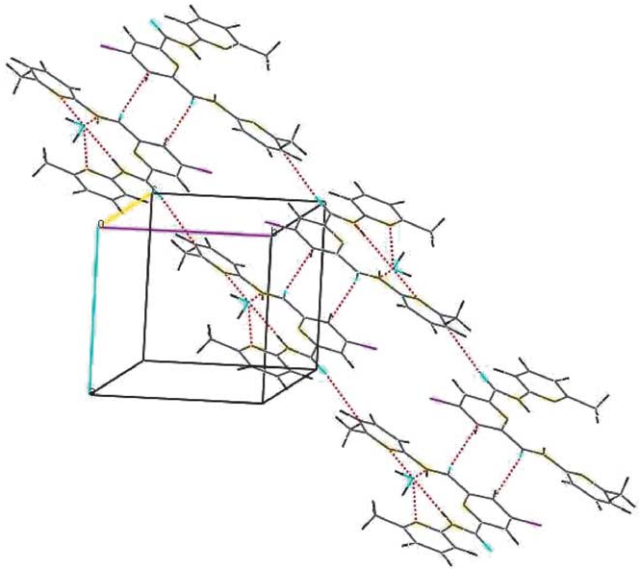

Figure 2. Dimers of Host **8** including a water molecule as a guest forming a ribbon. Dashed lines show hydrogen bonds.

A comparison of the molecular structure determined by X-ray crystallography with the structures obtained by molecular mechanics for the **8**:H_2O complex is reported in Table 5.

Table 5. Experimental and calculated geometries for **8**:H_2O

D (Å)/<(°)	X-Ray	AMBER	OPLS
N1···H17	2.26	2.18	2.14
N1···H8	2.20	2.24	2.13
N8–H8	1.00	1.02	1.02
O3···H8	2.13	1.87	1.86
N17–H17	0.95	1.02	1.02
O3···H17	2.15	1.88	1.85
O3–H3A	1.09	0.97	0.97
N10···H3A	2.04	2.12	2.13
O3–H3B	1.20	0.97	0.97
N19···H3B	1.76	2.08	2.14
N8–H8···O3	144.1	152.1	152.2
N17–H17···O3	154.9	154.3	152.5
O3–H3A···N10	129.2	143.6	138.8
O3–H3B···N19	140.5	137.7	138.2

Taking into account the difficulty to reproduce hydrogen bond interactions with molecular mechanics, the agreement is best than acceptable and gives confidence in both AMBER and OPLS optimised geometries.

2.3. Tautomerism pyridone/hydroxypyridine: compounds 9a/9b and 10a/10b

Before discussing the host–guest properties of the compounds under study, we will examine the pyridone (**a**)/hydroxypyridine (**b**) tautomerism of compounds **9** and **10** based on B3LYP/6-31G(d,p) calculations as well as the influence of a water molecule on these equilibria. Some of us have reported a theoretical study of the unsubstituted pyridone/hydroxypyridine equilibrium [B3LYP/6-31G(d)].[8] In the absence of any perturbation, 4-hydroxypyridine is more stable then 4-pyridone by 6.3 kJ mol^{-1}; the presence of two methyl ester substituents at positions 2,6 (the conformation of the arms was fixed to simulate the beginning of a crown ether), produces an inversion of the stability in favour of the pyridone by 6.5 kJ mol^{-1}. In the case of model compound **10** (fully optimisation, B3LYP/ 6-31G(d,p) and ZPE correction) the hydroxypyridine derivative **10b** is 30.2 kJ mol^{-1} more stable than **10a** (Scheme 6). This effect can be interpreted as due to the amide N–H groups that interact attractively with the lone pair on $N-1$ in the minimum conformation of **10b**. When the complexes formed by **10a** and **10b** with water are calculated, the energy difference becomes larger in favour of the hydroxy tautomer: **10b** $E_{rel}(+ZPE)=-61.2$ kJ mol^{-1} and **10a**, $E_{rel}(+ZPE)=0.0$ kJ mol^{-1}, as the conformation of the N,N'-dimethyl-2,6-dicarboxamides

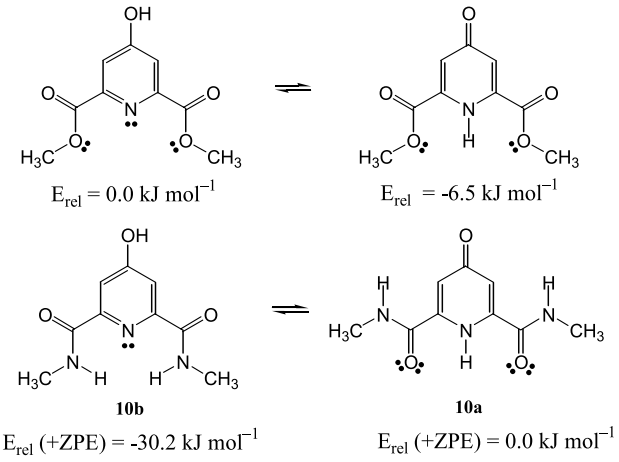

Scheme 6. The hydroxy/oxo tautomerism of pyridone derivatives taken from Ref. 8 (diesters) and from this work (diamides).

changes on formation of the complex **10a**:H_2O to include the water molecule into the cavity.

Although for compound **9** the calculations correspond to B3LYP/6-31G(d,p)//MM ones, tautomer **9b** is 167.3 kJ mol^{-1} more stable than **9a**, possibly due to the increased acidity of the N–H protons at position 2 of the pyridine ring. The 167.3 kJ mol^{-1} difference decreases to 111.3 kJ mol^{-1} if a water molecule is placed in the cavity of both **9a** and **9b** because the less stable tautomer **9a** is a better host for water than **9b**.

According to the B3LYP6-31G(d,p)//Monte Carlo Conformational Search, AMBER force field level calculations, the interaction energies of the four hosts with water (H_2O was always situated in the concave part) defined as $E_{complex} - (E_{host} + E_{water})$, are: +19.9 kJ mol^{-1} for **7** (destabilisation), −51.4 kJ mol^{-1} for **8** (stabilisation), −88.7 kJ mol^{-1} for **9a** (stabilisation), and −32.6 kJ mol^{-1} for **9b** (stabilisation). Note that **8**:H_2O fits the experimental X-ray structure (Fig. 1).

2.4. Experimental versus calculated binding constants

The interactions with guest **6** cannot be calculated with OPLS (Table 4), but it is possible to compare the AMBER and OPLS results for the remaining compounds. There is a rough proportionality between both series of values (Eq. (1)):

$$-E_{min}(\text{OPLS}) = (1.38 \pm 0.04) \times -E_{min}(\text{AMBER}), \quad (1)$$

$$n = 21, \quad r^2 = 0.983$$

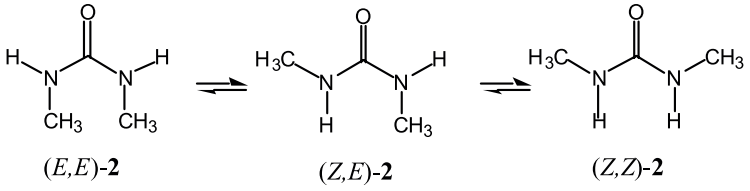

Scheme 7. The different conformations of *N*,*N*′-dimethylurea **2**.

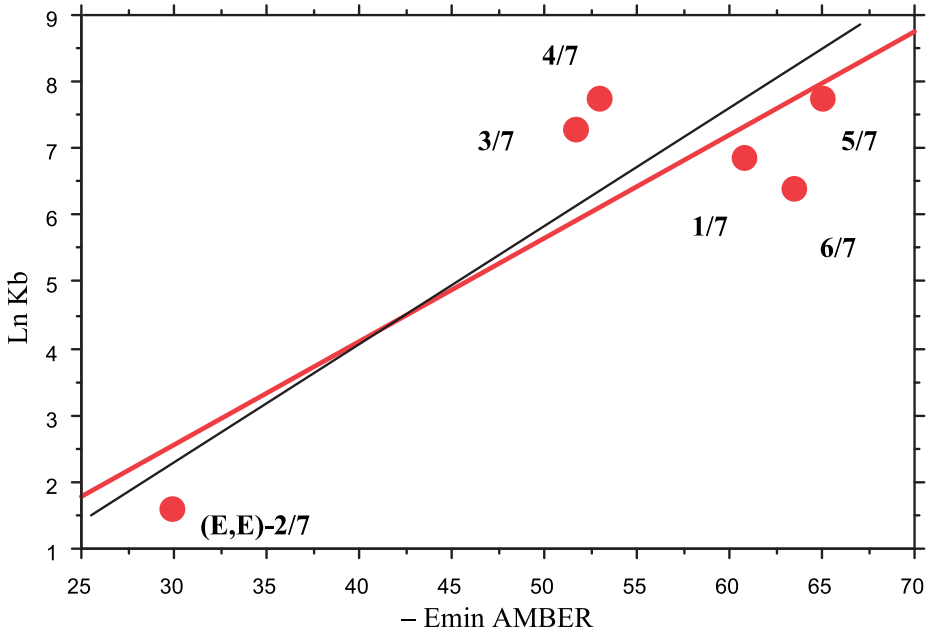

Figure 3. A plot the experimental results (Table 1) vs. the calculated ones (Table 3) for host **7**.

Comparison with the experimental results in the case of **7** is not good enough to discriminate between both kinds of calculations. Therefore, we will use the more complete AMBER values (Table 3).

When comparing the average K_b values for complexes of host **7** in Table 1 (after transforming them into Ln K_b) with $-E_{min}$ AMBER in Table 3, the first problem that arises is the isomerism of *N*,*N*′-dimethylurea **2** (Scheme 7). What of the three conformations of this compound is the most consistent with the experimental value?

Since the CIS are too small we have assumed an experimental value of $K_b=5$, and from the variation of ln K_b against $-E_{min}$ AMBER it appears that the (*E*,*E*)-**2** isomer is the one interacting with the host. For (*Z*,*E*)-**2** and (*Z*,*Z*)-**2** the residuals are much larger, so we have excluded these points in Fig. 3.

The red line corresponds to:

$$\text{Ln } K_b = -(2.1 \pm 2.6) + (0.155 \pm 0.047) \times -E_{min}(\text{AMBER}),$$

$$n = 6, \quad r^2 = 0.73 \tag{2}$$

Removing tolbutamide (**6**) one obtains the black line:

$$\text{Ln } K_b = -(2.9 \pm 2.5) + (0.176 \pm 0.047) \times -E_{min}(\text{AMBER}),$$

$$n = 5, \quad r^2 = 0.82 \tag{3}$$

We turn now to the data of host **8**. For homogeneity reasons we have based our discussion on the AMBER calculations of Table 3. Like in the preceding case, the best agreement in the case of guest **2** is found for the *E*,*E* conformation with an experimental K_b value of 5. Of the two columns for **8**, the results are better using the GB/SA model for water as shown in Fig. 4.

The blue line corresponds to:

$$\text{Ln } K_b = (0.8 \pm 1.4) + (0.083 \pm 0.024) \times -E_{min} \text{ AMBER (Water} - \text{GB/SA)}, \tag{4}$$

$$n = 6, \quad r^2 = 0.76$$

Here again, tolbutamide (**6**) is the worse point. Removing it one obtains as indicated in the black line:

$$\text{Ln } K_b = -(0.3 \pm 1.3) + (0.112 \pm 0.025) \times -E_{min} \text{ AMBER (Water} - \text{GB/SA)}, \tag{5}$$

$$n = 5, \quad r^2 = 0.87$$

It is possible to treat together hosts **7** and **8** using AMBER ($CHCl_3$-GB/SA) for **7** and AMBER (Water-GB/SA) for **8**:

Three regression lines can be calculated for the points of Fig. 5:

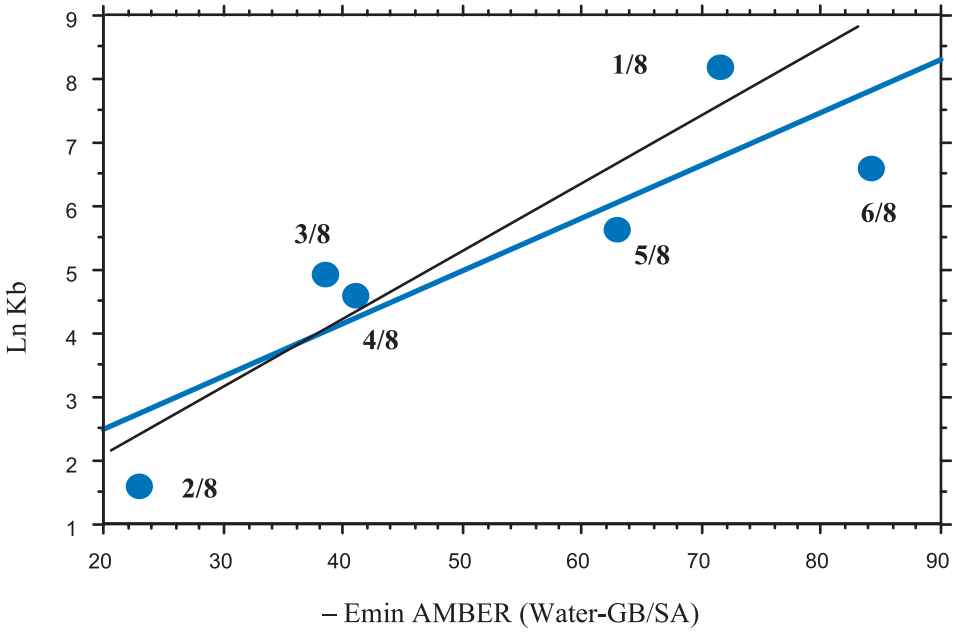

Figure 4. A plot the experimental results (Table 2) vs. the calculated ones (Table 3) for host **8**.

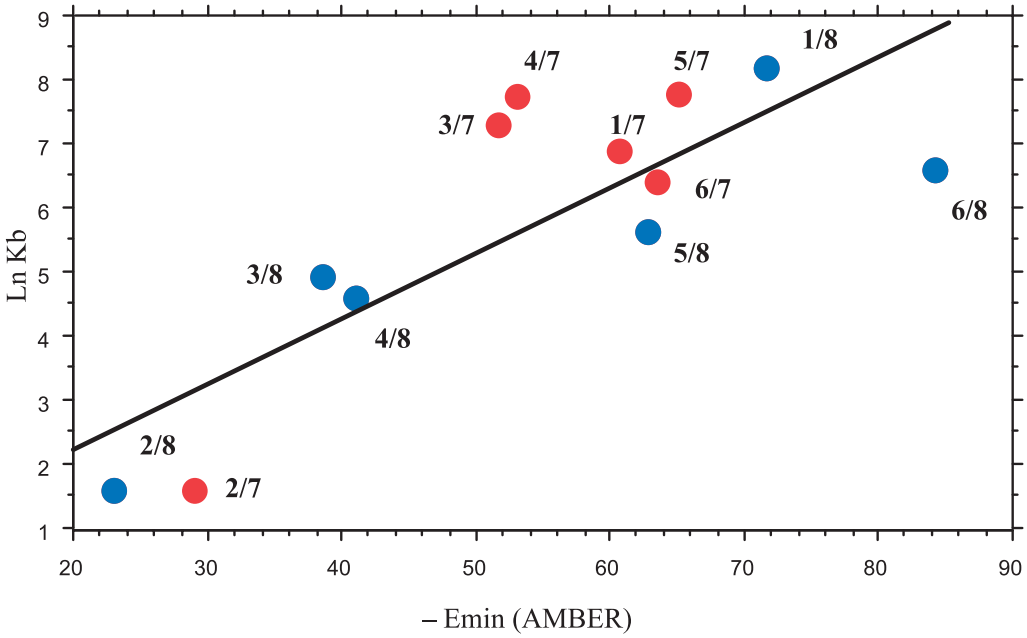

Figure 5. A plot the experimental results (Tables 1 and 2) vs. the calculated ones (Table 3) for hosts **7** and **8**.

$$\text{All points}: \text{Ln}\,K_b = (0.4 \pm 1.3) + (0.101 \pm 0.023) \times -E_{min}\ \text{AMBER}, \quad n = 12, \quad r^2 = 0.65 \tag{6}$$

$$\text{Without 6}: \text{Ln}\,K_b = -(1.1 \pm 1.2) + (0.135 \pm 0.023) \times -E_{min}\ \text{AMBER}, \quad n = 10, \quad r^2 = 0.81 \tag{7}$$

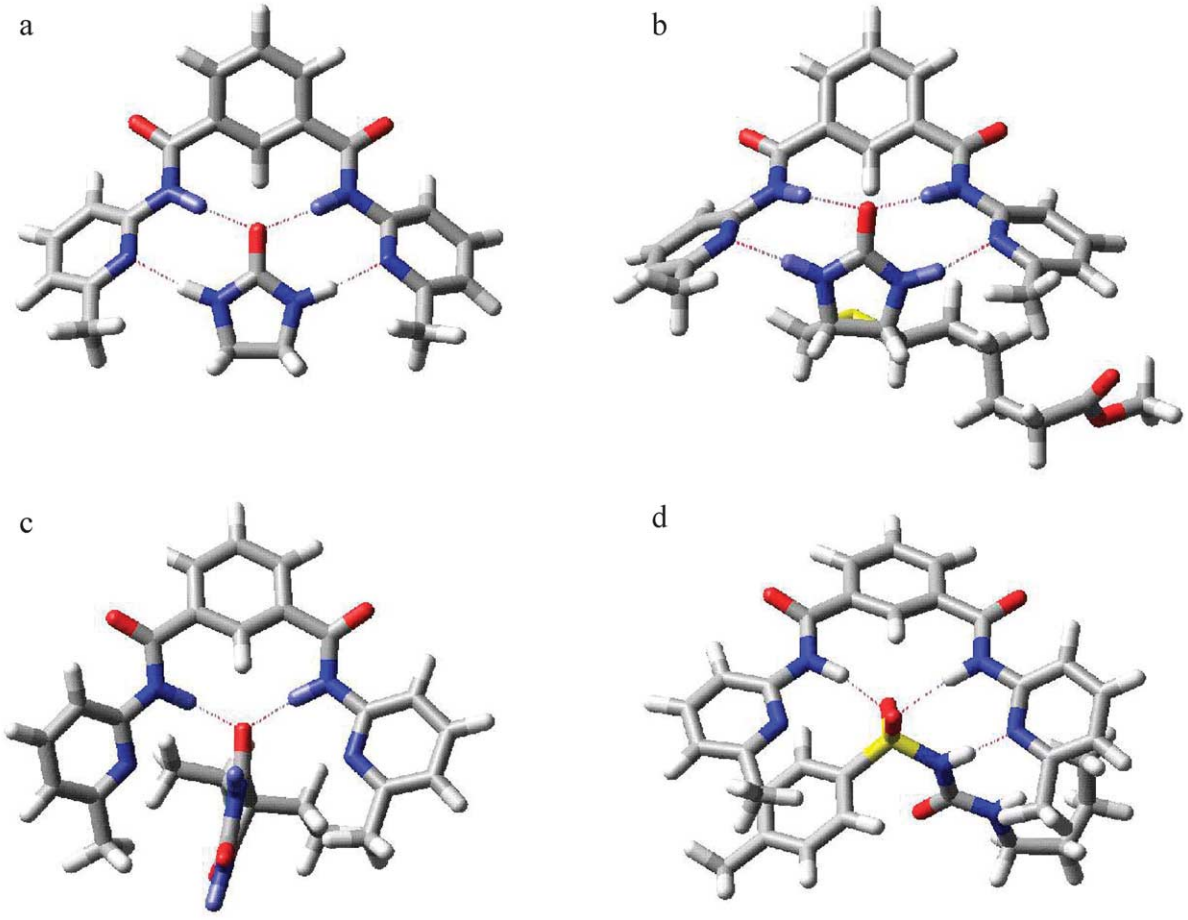

Figure 6. Structures of complexes: a. **7**:**3**; b. **7**:**1**; c. **7**:**5**; d. **7**:**6**.

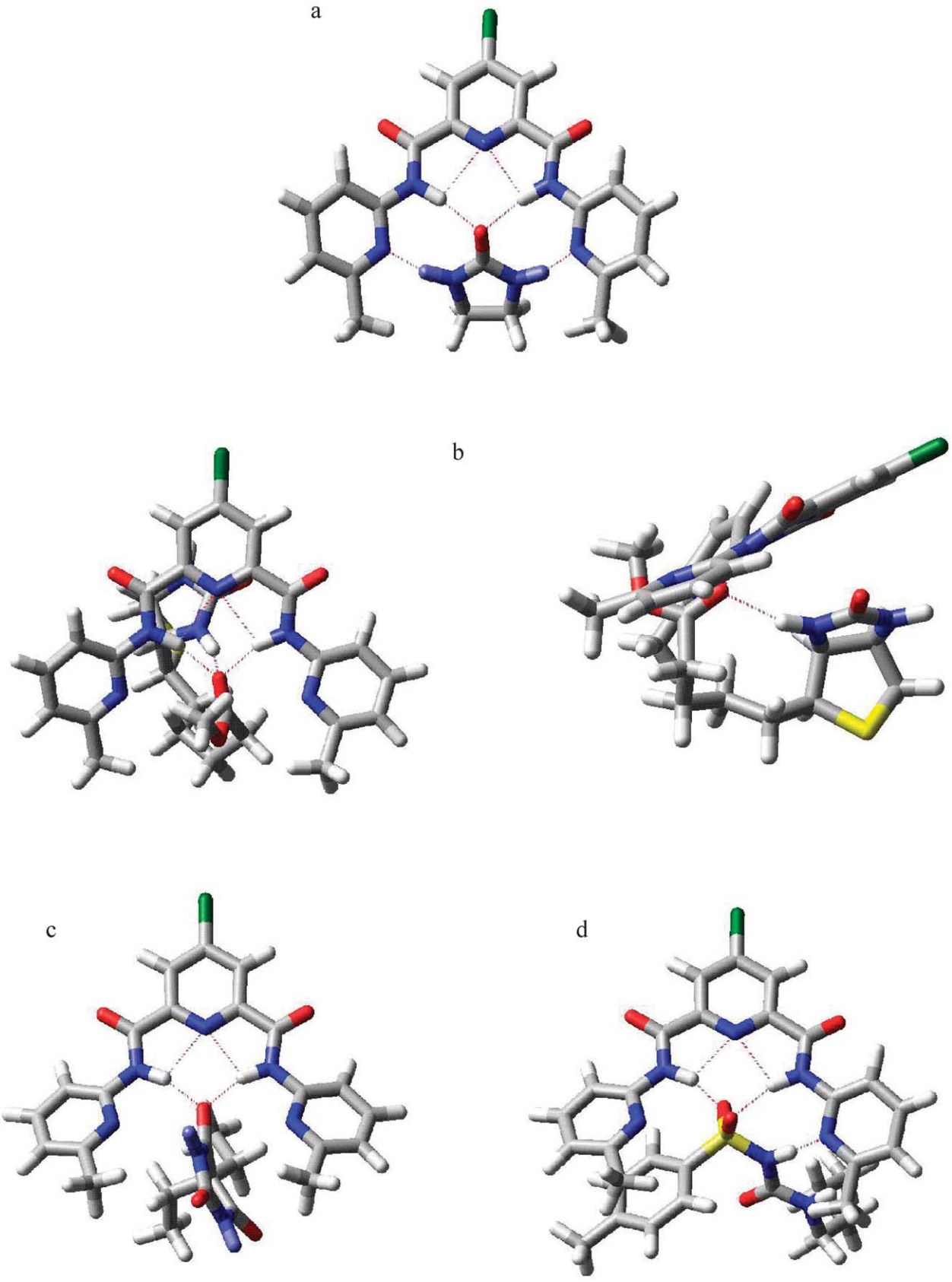

Figure 7. Structures of complexes: a. **8**:**3**; b.**8**:**1**; c. **8**:**5**; d. **8**:**6**.

No intercept : Ln $K_b = (0.115 \pm 0.007) \times -E_{min}$ AMBER,

$$n = 10, \quad r^2 = 0.97 \tag{8}$$

To explain why tolbutamide (**6**) deviates it is necessary to examine the structure of the complexes as calculated by AMBER for hosts **7** and **8**. If we consider the complex between **7** and 2-imidazolidone (**3**) (Fig. 6a) as representative of the studied complexes, we observe that those of biotin methyl ester (**1**) (Fig. 6b), *N*,*N*′-dimethylurea (**2**) in its *E*,*E*-conformation and trimethyleneurea (**4**) are very similar. That of barbital (**5**) uses only the carbonyl group (Fig. 6c) and tolbutamide (**6**) only the SO_2–NH moiety (Fig. 6d).

Similar features are found for host **8** (Fig. 7a–c), save in the case of biotin methyl ester (**1**) where no CIS were observed on the NH chemical shifts (Table 2) proving that there is no interaction through the urea moiety. The binding takes place involving the amide NHs of the host and the carbonyl group of the biotin side chain. In the two views of the structure of the complex **8**:**1** shown in Fig. 7b, that corresponds to the energy minimum, the two internal hydrogen bonds remain intact and there are no changes in the original conformations nor in the host neither in the guest.

The binding modes were confirmed in the complex of tolbutamide (**6**) with host **7** by means of NOESY NMR experiments that proved the closeness of the *p*-tolyl protons of **6** to the methyl group of the host (Fig. 8a) and the guest aliphatic chain protons to host pyridine ones (Fig. 8b). This information allowed us to calculate the new energy minimum of -63.4 kJ mol^{-1} depicted in Table 3, that fits the experimental binding constant K_b.

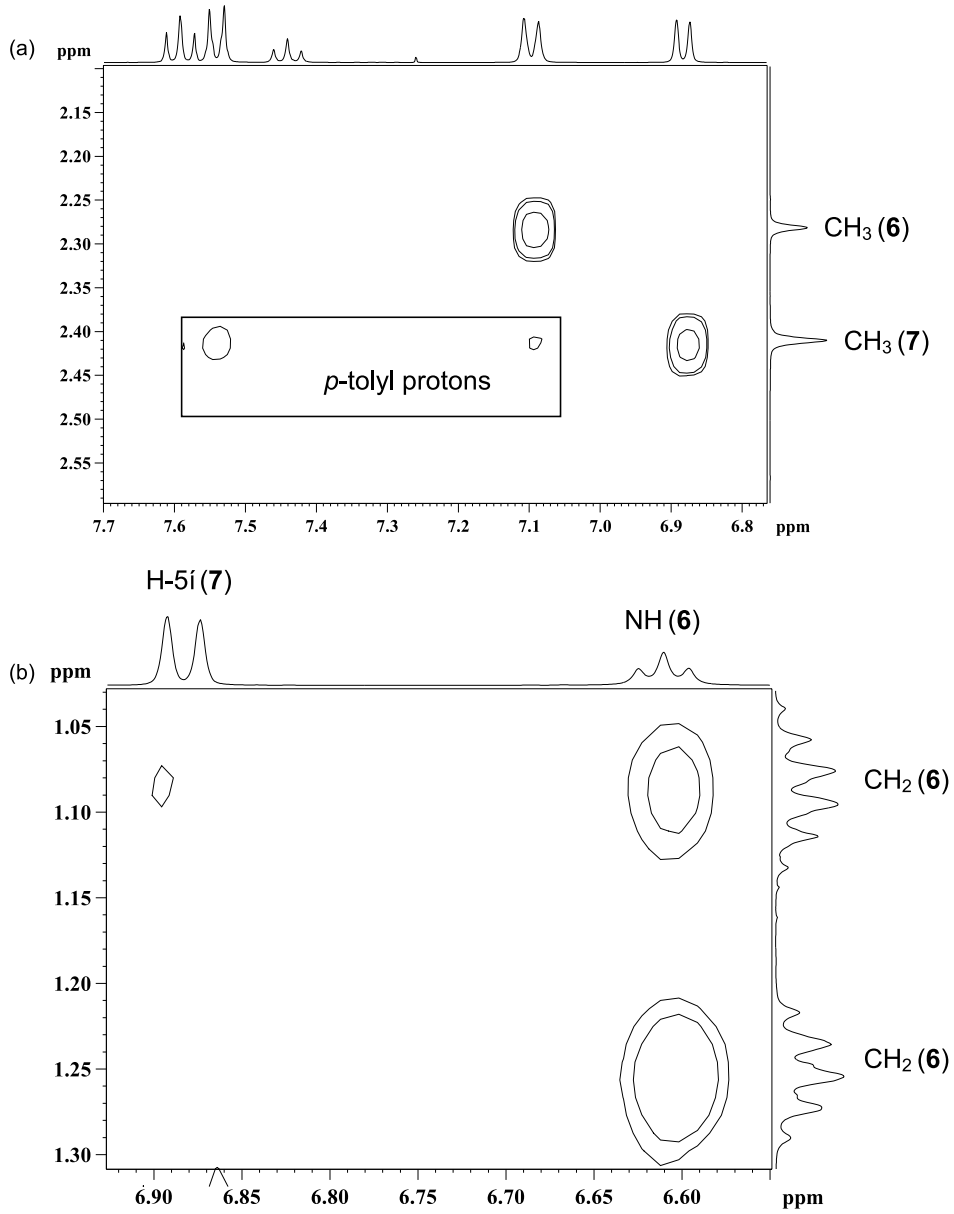

Figure 8. Enlarged regions of the NMR NOESY spectra.

Moreover, no changes in the ^{13}C NMR chemical shift of the urea carbonyl group of tolbutamide (**6**) are induced when complexes **7**:**6** and **8**:**6** are formed.

3. Conclusions

As a result of our studies, two different conformations in the complexation mode of biotin methyl ester (**1**) with **7** and **8** have been found. The conformation with **7** is similar to the normal one shown by the ureas, but with **8** is completely different and takes place through the carbonyl group of the biotin side chain. Concerning barbital (**5**), the hosts are only able to accommodate one part of the molecule but the K_b values are high (the highest with **7**), a similar observation was made with the hosts of our precedent paper.[1]

Tolbutamide (**6**) is rather different from the other five ureas because the sulfonyl group increases considerably the acidity of the contiguous NH[11] but also modifies the conformation. Based on its X-ray structure,[12] we have represented it in Scheme 2 with both NHs opposite to the C=O (like a *Z*,*Z*-dimethylurea). Although this is the conformation found in the complexes, tolbutamide is too different from classical ureas to fit well in the same series of calculations.

4. Experimental

4.1. General

The six guests are commercially available: biotin methyl ester (**1**) (>99%, dried under vacuum), *N*,*N*′-dimethylurea (**2**) (99%, recrystallized from ethyl acetate), 2-imidazolidone (**3**) (96%, recrystallized from ethyl acetate), *N*,*N*′-trimethyleneurea (**4**) (>98%, recrystallized from ethyl acetate), barbital (**5**) (>99%) and tolbutamide (**6**) (>99%). Melting points were determined in a Thermo-Galen hot stage microscope and are uncorrected. Elemental analyses for carbon, hydrogen, and nitrogen were carried out by the Microanalytical Service of the Complutense University on a Perkin-Elmer 240 analyser.

4.2. NMR spectroscopy

NMR spectra were recorded on a Bruker DRX 400 (9.4 T, 400.13 MHz for ^1H, 100.62 MHz for ^{13}C and 40.56 MHz for ^{15}N) spectrometer at 300 K. Chemical shifts (δ in ppm) are given from internal solvent $CDCl_3$ 7.26 for ^1H and 77.0 for ^{13}C, DMSO-d_6 2.49 for ^1H and 39.5 for ^{13}C and for ^{15}N NMR nitromethane was used as external standard. Coupling constants (J in Hz) are accurate to $J=\pm0.2$ Hz for ^1H and ^{13}C and $J=\pm0.6$ Hz for ^{15}N. 2D-Inverse proton detected homonuclear shift correlation spectra gs-COSY (^1H–^1H), NOESY and 2D inverse proton detected heteronuclear shift correlation spectra, gs-HMQC (^1H–^{13}C), gs-HMBC (^1H–^{13}C) and gs-HMBC (^1H–^{15}N), were carried out with the standard pulse sequences to assign the ^1H, ^{13}C and ^{15}N signals.

4.3. Synthesis of *N*,*N*′-bis(6-methylpyridin-2-yl)-1,3-benzenedicarboxamide (7)

See Scheme 4. Isophthaloyl chloride (**11**, 1 g, 4.9 mmol) was dissolved, under Ar, in 100 mL of dry CH_2Cl_2, then a solution of 2-amino-6-methylpyridine (**12**, 1.1 g, 9.9 mmol) and Et_3N freshly distilled (4 mL) in 90 mL of dry CH_2Cl_2 was added slowly from a pressure-equalising addition funnel. The resulting solution was stirred for 4 h and then washed with saturated solution of $NaHCO_3$ and water, dried (Na_2SO_4) and concentrated to yield a yellow-pale solid which is recrystallized from MeOH to obtain 0.74 g (44%) of **7**, mp 230 °C. ^1H NMR ($CDCl_3$): δ (ppm) 8.81 (broad s, 2H, NH), 8.48 (dd, 1H, H-2, $J_{2,4}=J_{2,6}=1.8$ Hz), 8.16 (d, 2H, H-3′, $J_{3',4}=8.2$ Hz), 8.10 (dd, 2H, H-4/H-6, $J_{4,5/6,5}=7.8$ Hz), 7.63 (dd, 2H, H-4′, $J_{4',5'}=7.7$ Hz), 7.58 (dd, 1H, H-5), 6.92 (d, 2H, H-5′), 2.42 (s, 6H, CH_3). ^{13}C NMR ($CDCl_3$): δ (ppm) 164.5 (CO), 156.9 (C6′), 150.5 (C2′, $^3J=9.2$ Hz), 138.9 (C4′, $^1J=161.0$ Hz), 135.0 (C1/C3, $^3J=7.7$ Hz), 130.8 (C4/C6, $^1J=161.8$ Hz, $^3J=6.1$ Hz), 129.4 (C5, $^1J=162.6$ Hz), 125.9 (C2, $^1J=161.0$ Hz, $^3J=6.1$ Hz), 119.7 (C5′, $^1J=162.6$ Hz, $^3J=6.2$ Hz), 111.0 (C3′, $^1J=171.8$ Hz, $^3J=6.1$ Hz), 23.9 (CH_3, $^1J=127.3$ Hz, $^3J=3.1$ Hz). ^{15}N NMR ($CDCl_3$): δ (ppm) −242.9 (NH), −98.9 (N1′). Anal. Calcd for $C_{20}H_{18}N_4O_2$: C, 69.35; H, 5.24; N, 16.17%. Found: C, 69.09; H, 5.29; N, 16.09%.

4.4. Synthesis of 4-chloro-*N*,*N*′-bis(6-methylpyridin-2-yl)-2,6-pyridindicarboxamide (8)

See Scheme 5. Chelidamic acid (**13**, 0.5 g, 2.73 mmol) is dissolved in thionyl chloride (10 mL, 137.4 mmol) with the minimum quantity of DMF and the solution is heated at 110 °C for 3 h. After that, DMF and thionyl chloride are evaporated at reduce pressure until a white solid of 4-chlorochelidamic acid dichloride (**15**) is obtained, 0.45 g (74%), mp 200 °C. ^1H NMR (DMSO-d_6): δ (ppm) 8.46 (s, 2H, H3/H5).

4-Chlorochelidamic acid dichloride (**15**, 0.5 g, 2.10 mmol) was dissolved, under Ar, in 20 mL of dry CH_2Cl_2, then a solution of 2-amino-6-methylpyridine (**12**, 0.68 g, 4.55 mmol) and Et_3N freshly distilled (3 mL) in 30 mL of dry CH_2Cl_2 was added slowly from a pressure-equalising addition funnel. The resulting solution was stirred for 4 h and then washed with saturated solution of $NaHCO_3$ and water, dried (Na_2SO_4) and concentrated to yield a white solid which is recrystallized from MeOH to obtain 0.35 g (40%) of **8**, mp 244 °C. ^1H NMR ($CDCl_3$): δ (ppm) 10.23 (broad s, 2H, NH), 8.46 (s, 2H, H-3/H-5), 8.20 (d, 2H, H-3′, $J_{3',4'}=8.2$ Hz), 7.67 (dd, 2H, H-4′, $J_{4',5}=7.5$ Hz), 6.98 (d, 2H, H-5′), 2.52 (s, 6H, CH_3). ^{13}C NMR ($CDCl_3$): δ (ppm) 160.5 (CO), 157.2 (C6′), 150.2 (C2/C6), 150.0 (C2′, $^3J=9.2$ Hz), 148.3 (C4, $^2J=3.1$ Hz), 138.8 (C4′, $^1J=161.0$ Hz), 126.1 (C3/C5, $^1J=174.6$ Hz, $^3J=4.5$ Hz), 119.9 (C5′, $^1J=162.9$ Hz, $^3J=6.1$ Hz), 111.3 (C3′, $^1J=171.6$ Hz, $^3J=6.1$ Hz), 24.0 (CH_3, $^1J=127.3$ Hz). ^{15}N NMR ($CDCl_3$): δ (ppm) −247.1 (NH), −97.9 (N1′), −97.2 (N1). Anal. Calcd for $C_{19}H_{16}ClN_5O_2\cdot H_2O$: C, 57.07; H, 4.54; N, 17.52%. Found: C, 57.17; H, 4.67; N, 17.49%.

4.5. NMR titrations

Each NMR titration was carried out at least three times at 300 K in $CDCl_3$ as a solvent (Merck S33657, deuterium content >99.8%, water content <0.01%). The syringes are from Hamilton–Bonaduz, 5 μL (divisions 0.05 μL), 10 μL (divisions 0.1 μL), 250 μL (divisions 5 μL) and the balance for weighting the host and the guest a Metler AE260-Delta Range (error ±0.00005 g). ^{1}H NMR titrations are used in order to quantify K_b values, these titrations are carried out following the Chemical Induced Shift (CIS) in one or several protons of host or guest while the concentration of the complex formed is changed by the addition of one of the components. For host **7** we performed a double independent quantification following the CIS for amide protons and the H-2 in the central benzene ring, while guest solution aliquots are added. There are a large number of ways to fit the data from a titration,[9] but that consisting in non-linear curve fitting is generally accepted as the method with the lowest error in the determination of K_b values, in comparison to others that employ approximations to reach a linear relationship between δ and K_b. To fit the experimental data the Sigmaplot 8.1 program from SPSS Science Software Gmbh was employed. The basic equation used in this kind of titrations is represented by [Eq. (9)], showing the relationship between chemical shifts (δ), concentrations of host H, guest G and complex C, and the binding constant $K_b=[C]/([H][G])$, this equation is valid only for 1:1 stoichiometry as is our case.[10]

$$\delta_{OBS} = (\delta_C - \delta_H)(\{(1 + [G]/[H] + 1/Kb[H])/2\} - \{(1 + [G]/[H] + 1/K_b[H])^2/4 - [G]/[H]\}^{1/2}) + \delta_H \quad (9)$$

In order to obtain K_b values with the lowest error the titrations are carried out in the 20–80% saturation range for the compound which CIS is being followed. This condition determines the concentrations to be used in the titrations for both host and guest and a calculation has to be done to find those concentrations that best cover the whole range of p in order to get the maximum information from the titration curve. The accuracy in the concentration range to be used in titrations is usually disregarded in most publications of the host–guest field, affording K_b values totally different from those obtained following this procedure. The error determined by this magnitude is intrinsic to the measurement method and it is not reflected by the standard deviation (S_d) which is a measure of the fit goodness of the data employed.

The titrations for the complex between host **8** and water are carried out on the same way (20–80% saturation range), water concentration is determined by the integration of its NMR signal. The host sample for the titration is prepared with freshly distilled $CDCl_3$ and molecular sieve 4 Å is added to keep water at the minimum concentration, on this way all the samples had an initial saturation range between 20–30%, so the titration was carried out in the right saturation range. The results were reported in Table 2.

Titrations between host **8** and biotin methyl ester (**1**) are carried out by the same method but keeping the concentration of water under 1 mM in order to avoid a competitive behaviour of the water.[5]

For guests **3**, **4**, **5** and **6** a competitive titration is used, the CIS of the two guests are measured while aliquots of the host are added. The fitting of the data to the (Eq. (10)) allows to obtain a relative K_b for the guest we are studying, as the K_b for the complex **8**:water was previously measured we can calculate the value for the complex **8**:guest.

$$K_{b(water)}/K_{b(guest)} = [(1/F_{guest}) - 1]/[(1/F_{water}) - 1] \quad (10)$$

F_{water} and F_{guest} are the molar fractions of water and guest that are bound to the host, if no another equilibria arise (which it has been proved with titrations of the guest versus water), then $F_i=(\delta_{i,Free}-\delta_{iObserved})/(\delta_{i,Free}-\delta_{i,Complexed})$.

4.6. MM calculations

MacroModel v.8.1, with the GB/SA model for chloroform[13] was used in order to perform the molecular simulations of the complexes in all cases, save as indicated in Table 3. All calculations were achieved with Monte Carlo (MC) conformational analyses.[14] Minimisation is carried out using Polak-Ribiere conjugate gradient optimiser.[15] In a typical MC run a MCMM is performed with never less than 8000 steps, to carry out the search both torsional rotations in host and guest and translation/rotation (10 Å/360°) of the guest is performed, for all the MC a cutoff is applied to van der Waals, electrostatic and H-bond interactions with 7, 12 and 4 Å, respectively. These calculations were carried out with two different force fields, AMBER*,[16] and OPLS*,[17] as implemented in the version of the program.

4.7. DFT calculations

Single point calculations were carried out at the B3LYP/6-31G(d,p) level of theory[18,19] with the Gaussian '03 program on the optimised Molecular Mechanics geometries.[20] At this level we calculated the energies for the complexes between hosts **7**, **8** and **9a/9b** with water, analysing the energy differences between the two possible tautomers in host **9** (**a**, 4-pyridone/**b**, 4-hydroxypyridine). BSSE were determined for all the complexes computed by DFT with the counterpoise correction.[21]

Model compound **10a/10b** and its water complexes were fully optimised (no imaginary frequencies).

4.8. Crystallographic data collection and structure determination of 8a:H_2O

Suitable crystal for X-ray diffraction experiments was obtained by crystallization from acetone/hexane. Data collection was carried out at room temperature on a Bruker Smart CCD diffractometer using graphite-monochromated Mo K(radiation (λ=0.71073 Å) operating at 50 Kv and 30 mA. Data were collected over a hemisphere of the reciprocal space by combination of three exposure sets. Each exposure of 30 s covered 0.3 in ω. Structure was

Table 6. Crystal data and structure refinement for **8**:H_2O

Empirical formula	$C_{19}H_{18}ClN_5O_3$	
Formula weight	399.83	
Temperature	293(2) K	
Crystal system	Triclinic	
Space group	P-1	
Unit cell dimensions	$a=8.274(2)$ Å	$\alpha=114.003(5)°$
	$b=10.560(3)$ Å	$\beta=91.997(5)°$
	$c=11.942(3)$ Å	$\gamma=94.132(6)°$
Volume	948.4(4) Å^3	
Z	2	
Density (calculated)	1.400 Mg/m^3	
Absorption coefficient	0.233 mm^{-1}	
$F(000)$	416	
θ (°)	1.87–25.00°	
Index ranges	$-9\leq h\leq 9$,	
	$-10\leq k\leq 12$,	
	$-14\leq l\leq 13$	
Reflections collected	5030	
Independent reflections	3315 [R(int)=0.0494]	
Data/restraints/parameters	3315/0/255	
G.o.f. (F^2)	0.815	
R_1 [$I>2$sigma(I)][a]	0.0489 (ref. obs. 1342)	
R_2 (all data)[b]	0.1228	

[a] $\Sigma[|F_o|-|F_c|]\ /\Sigma|F_o|$.
[b] $\{\Sigma[w(F_o^2-F_c^2)^2]\ /\Sigma[w(F_o^2)^2]\}^{1/2}$.

solved by direct methods and refined by full-matrix least-square procedures on F^2 (SHELX-97).[22]

All non-hydrogen atoms were refined anisotropically. All hydrogen atoms were located in a difference Fourier map, included and fixed. Crystal data and other structure determination details are presented in Table 6.

CCDC-256026 contains the supplementary crystallographic data for this paper. These data can be obtained free of charge via www.ccdc.cam.ac.uk/conts/retrieving.html (or from the Cambridge Crystallographic Data centre, 12 union Road, Cambridge CB2 1EZ, UK; fax: (+44) 1223-336033; or www.deposit@ccdc.cam.uk.

Acknowledgements

Thanks are given to MCyT for financial support (project BQU2003-00976). One of us (F.H.) is grateful to the MCyT for a FPI fellowship.

References and notes

1. Claramunt, R. M.; Herranz, F.; Santa María, M. D.; Jaime, C.; de Federico, M.; Elguero, J. *Biosensors Bioelectron.* **2004**, *20*, 1242–1249.
2. Hedge, V.; Hung, C.-Y.; Madhukar, P.; Cunningham, R.; Höpfner, T.; Thummel, R. P. *J. Am. Chem. Soc.* **1993**, *115*, 872–878.
3. Goswami, S.; Mukherjee, R. *Tetrahedron Lett.* **1997**, *38*, 1619–1622.
4. Kecskemeti, V.; Bagi, Z.; Pacher, P.; Posa, I.; Kocsis, E.; Koltai, M. Z. *Curr. Med. Chem.* **2002**, *9*, 53–71.
5. Adrian, J. C.; Wilcox, C. S. *J. Am. Chem. Soc.* **1991**, *113*, 678–680.
6. Hirao, T.; Moriuchi, T.; Ishikawa, T.; Nishimura, K.; Mikami, S.; Ohshiro, Y.; Ikeda, I. *J. Mol. Catal. A* **1996**, *113*, 117–130.
7. Jouaiti, A.; Hosseini, M. W.; Kyritsakas, N. *Chem. Commun.* **2003**, 1898–1899.
8. Alkorta, I.; Elguero *J. Heterocycl. Chem.* **2001**, *38*, 1387–1391.
9. Fielding, L. *Tetrahedron* **2000**, *56*, 6151–6170.
10. Hirose, K. *J. Incl. Phenom. Macrocycl. Chem.* **2001**, *39*, 193–209.
11. NH-acidity (pK_a): tolbutamide: 5.3, barbital: 7.7: www.medchem.ku.edu/MDCM625.
12. Nirmala, K. A.; Gowda, D. S. S. *Acta Crystallogr. Sect. B* **1981**, *37B*, 1597–1599. Donaldson, J. D.; Leary, J. R.; Ross, S. D.; Thomas, M. J. K.; Smith, C. H. *Acta Crystallogr. Sect. B* **1981**, *37B*, 2245–2248.
13. MacroModel, Schrödinger LLC, 2004. http://www.schrodinger.com/Products/macromodel.html.
14. Chang, G.; Guida, W. C.; Still, W. C. *J. Am. Chem. Soc.* **1999**, *111*, 4379–4385.
15. Polak, E. Computational Methods in Optimization; Academic Press: New York, 1971. Brodlie, K. W. In *The State of the Art in Numerical Analysis*; Jacobs, D. A. H., Ed.; Academic Press: London, 1977; Chapter III. 1.7.
16. Weiner, P. K.; Kollmann, P. A. *J. Comput. Chem.* **1981**, *2*, 287–303.
17. Jorgensen, W. L.; Tirado-Rives *J. Am. Chem. Soc.* **1998**, *110*, 1657–1664.
18. Becke, A. D. *Phys. Rev. A* **1988**, *38*, 3098–3100. Becke, A. D. *J. Chem. Phys.* **1993**, *98*, 5648–5652. Lee, C.; Yang, W.; Parr, R. G. *Phys. Rev. B* **1988**, *37*, 785–789. Miehlich, B.; Savin, A.; Stoll, H.; Preuss, H. *Chem. Phys. Lett.* **1989**, *157*, 200–206.
19. Ditchfield, R.; Hehre, W. J.; Pople, J. A. *J. Chem. Phys.* **1971**, *54*, 724–728.
20. Gaussian 03, Revision B.04, Frisch, M. J.; Trucks, G. W.; Schlegel, H. B.; Scuseria, G. E.; Robb, M. A.; Cheeseman, J. R.; Montgomery, J. A. Jr.; Vreven, T.; Kudin, K. N.; Burant, J. C.; Millam, J. M.; Iyengar, S. S.; Tomasi, J.; Barone, V.; Mennucci, B.; Cossi, M.; Scalmani, G.; Rega, N.; Petersson, G. A.; Nakatsuji, H.; Hada, M.; Ehara, M.; Toyota, K.; Fukuda, R.; Hasegawa, J.; Ishida, M.; Nakajima, T.; Honda, Y.; Kitao, O.; Nakai, H.; Klene, M.; Li, X.; Knox, J. E.; Hratchian, H. P.; Cross, J. B.; Adamo, C.; Jaramillo, J.; Gomperts, R.; Stratmann, R. E.; Yazyev, O.; Austin, A. J.; Cammi, R.; Pomelli, C.; Ochterski, J. W.; Ayala, P. Y.; Morokuma, K.; Voth, G. A.; Salvador, P.; Dannenberg, J. J.; Zakrzewski, V. G.; Dapprich, S.; Daniels, A. D.; Strain, M. C.; Farkas, O.; Malick, D. K.; Rabuck, A. D.; Raghavachari, K.; Foresman, J. B.; Ortiz, J. V.; Cui, Q.; Baboul, A. G.; Clifford, S.; Cioslowski, J.; Stefanov, B. B.; Liu, G.; Liashenko, A.; Piskorz, P.; Komaromi, I.; Martin, R. L.; Fox, D. J.; Keith, T.; Al-Laham, M. A.; Peng, C. Y.; Nanayakkara, A.; Challacombe, M.; Gill, P.M. W.; Johnson, B.; Chen, W.; Wong, M. W.; Gonzalez, C.; Pople, J. A. Gaussian, Inc., Pittsburgh PA, 2003.
21. Boys, S. B.; Bernardi, F. *Mol. Phys.* **1970**, *19*, 553–558.
22. Sheldrick, G.M. SHELX97, Program for Refinement of Crystal Structure, University of Göttingen, Göttingen, Germany, 1997.